

Minimum loading requirements for areas of low seismicity

Nelson T.K. Lam^{*1,3}, Hing-Ho Tsang^{2,3a}, Elisa Lumantarna^{1,3b}
and John L. Wilson^{2,3c}

¹Department of Infrastructure Engineering, The University of Melbourne,
Parkville, Victoria, Australia

²Faculty of Science, Engineering and Technology, Swinburne University of Technology,
Melbourne, Victoria, Australia

³Bushfire and Natural Hazards Cooperative Research Centre, Melbourne, Australia

(Received November 11, 2015, Revised September 25, 2016, Accepted September 27, 2016)

Abstract. The rate of occurrence of intraplate earthquake events has been surveyed around the globe to ascertain the average level of intraplate seismic activities on land. Elastic response spectra corresponding to various levels of averaged (uniform) seismicity for a return period of 2475 years have then been derived along with modifying factors that can be used to infer ground motion and spectral response parameters for other return period values. Estimates derived from the assumption of uniform seismicity are intended to identify the minimum level of design seismic hazard in intraplate regions. The probabilistic seismic hazard assessment presented in the paper involved the use of ground motion models that have been developed for regions of different tectonic and crustal classifications. The proposed minimum earthquake loading model is illustrated by the case study of Peninsular Malaysia which has been identified with a minimum effective peak ground acceleration (EPGA) of 0.1 g for a return period of 2475 years, or 0.07 g for a notional return period of 475 years.

Keywords: intraplate earthquake; response spectrum; return period; uniform seismicity; Malaysia

1. Introduction

Probabilistic seismic hazard assessment (PSHA) which was first introduced by Cornell-McGuire (Cornell 1968, McGuire 1976) has become universally accepted practice for quantifying the level of seismic hazard. As introduced in almost every textbook on earthquake risk assessments (e.g., Dowrick 2009), Cornell-McGuire PSHA procedure is resolved into four key steps namely: (i) identification of potential seismic sources; (ii) characterisation of each seismic source by magnitude recurrence modelling; (iii) ground motion predictions for all considered earthquake scenarios; and (iv) integration of contributions from multiple sources with the considerations of both aleatory and epistemic uncertainties. The spatial distribution of hazard

*Corresponding author, Associate Professor, E-mail: ntkl@unimelb.edu.au

^aSenior Lecturer, E-mail: htsang@swin.edu.au

^bLecturer, E-mail: elu@unimelb.edu.au

^cProfessor, E-mail: jwilson@swin.edu.au

levels obtained from this assessment procedure is usually presented in the form of contour maps which become an integral part of a seismic design standard.

Alternative PSHA procedures have been proposed by various researchers over the last two decades with the aim of enhancing the robustness of hazard estimates (e.g., McGuire 1993, Frankel 1995, Kijko and Graham 1999, Tsang and Chandler 2006, Tsang *et al.* 2011). However, all PSHA procedures are based mainly on the premise that the location of past events should be indicative of the location of potential hazards for the future. This has been found to be true to a certain extent in some evaluation studies (Kafka 2007, Camelbeeck *et al.* 2007) but is very dependent on the sample of data being sufficiently large to capture the underlying long term trends.

Whilst the philosophy of PSHA is straightforward and the procedure as a whole is well known, important discretionary judgment needs to be exercised in every step of the modelling (particularly step (i)) in lower seismic regions where few data points are available. The assumptions and judgment made are usually not well justified on scientific grounds (Stein *et al.* 2011). It has been reported that earthquake motions recorded from all around the world exceeded those indicated in seismic hazard maps more frequently than expected (Tsang 2011). Many large and destructive earthquakes have occurred on unrecognised faults (e.g., 1994 Northridge earthquake) or in places that were considered relatively low hazard, including the 1995 Kobe earthquake (Chandler 1997), 2003 Algeria earthquake, 2008 Wenchuan earthquake (Tsang 2008), 2010 Haiti earthquake, and 2011 Tohoku earthquake (Kerr 2011). The huge residual risk is highlighted in the discrepancies between the actual and expected numbers of fatalities (Wyss *et al.* 2012).

In regions of low-to-moderate seismicity the number of historical earthquake events that have a magnitude ($M > 4$) that exceeds the threshold of causing structural damage is sparse. Thus, a finely divided source zone model (using a conventional PSHA) in such a region would predict a high level of hazard in areas where earthquakes had occurred. The main concern with this modelling approach is the underestimation of seismic hazard in areas where the historical database has not shown any local seismic activity or no fault structure has been found. Consequently, areas where tremors have never been recorded on the historical archive can be interpreted to be having a nominal level of seismic hazard. Examples of such areas can be found in many parts of Australia (GA 2012), Peninsular Malaysia (Pappin *et al.* 2011) and the island of Sri Lanka (Venkatesan *et al.* 2015).

Intraplate seismicity by definition exists in all areas away from any tectonic plate margins. Thus, earthquake events are possible at virtually any place on earth (Bird *et al.* 2010). Some of these areas show little sign of activities if the period of observation is not sufficiently long or the catchment area is too small. It was revealed in simulation studies undertaken by Swafford and Stein (2007) that it could take thousands of years of seismological monitoring to capture the underlying spatial pattern of seismicity in an intraplate area where the rate of crustal deformation is 2 - 3 orders of magnitude lower than in interplate regions. Consequently, defining areas in an intraplate region where earthquake tremors have never been recorded as “earthquake free” significantly discounts the actual underlying hazard, and risk. For example, for areas such as Peninsular Malaysia where there has been no $M > 5$ event recorded in the past 50 years the level of seismicity cannot be discounted to zero, similarly for the island state of Singapore and Sri Lanka. Unfortunately, there is no general consensus over the minimum threshold (baseline) hazard that should be adopted for structural design in these areas to account for intraplate seismicity.

The alternative broad source zone modelling approach predicts a uniform level of hazard and fails to identify “hot spots” of relatively high seismic activities within an intraplate region. The

authors support continuing the practice of using conventional PSHA for predicting spatial variation of seismic hazard surrounding areas where earthquakes have occurred. At the same time, and importantly, a broad source zone modelling approach should be adopted as well to establish the minimum hazard level. The latter approach is the subject matter of this paper.

Both the finely divided source zone and the broad source zone PSHA modelling approach, when used on their own, would run the risk of understating seismic hazard in certain areas even if results derived from the two models are weighted by the *logic tree*. Essentially, the two modelling approaches should be considered as separate “*load cases*” to be considered which is a common terminology used in engineering design. The concept of *load cases* in the context of seismic hazard modelling should not be confused with the established concept of multiple seismic source models. The latter methodology used in PSHA involves the use of the *logic tree* to weigh results whereas the proposed *load case* approach of a broad source zone that considers average seismic activities controls the minimum level of hazard irrespective of results generated from other load cases.

The concept of minimum (commonly referred as “background”) seismicity is not new and is a recognised phenomenon in intraplate regions. What is needed for now is a rational basis of quantifying the rate of earthquake recurrence and the corresponding level of background hazard for use in engineering design. The objective of this paper is to present the derivation of the background hazard using recurrence rates of intraplate earthquakes from around the world. The rate of recurrences of earthquakes from a number of countries, and areas, away from tectonic plate boundaries was first surveyed to estimate the average level of intraplate earthquake activity (Section 2). The computational aspects of the PSHA methodology for predicting seismic hazard generated from a broad source zone is then presented (Section 3). Response spectral values at 0.3 s and 1.0 s as derived from PSHA of *broad source zones* are then presented for a range of ground motion models including those that are specifically intended to be used to represent intraplate earthquakes (Section 4). Finally, the use of the proposed minimum earthquake loading model is illustrated with the case study of *Peninsular Malaysia* where local seismicity data is too limited to apply *PSHA* in the conventional manner (Section 5).

2. Global rate of recurrences of intraplate earthquakes

The investigation into establishing the recurrence rate of intraplate earthquakes first focused on counting earthquake events occurring on land in stable continental areas away from the tectonic plate boundaries. Earthquakes exceeding magnitude 5 were used in the counting process since the records are more complete and the intraplate hazard is contributed mainly by events in the range M5 - M6.

It is noted that global *b*-values are typically in the range of 0.75 - 1.1 and have been found to vary depending on the region and the faulting mechanism (Heety 2011). The *b*-value was estimated to be around 0.93 on average for earthquakes featuring a thrust-faulting mechanism which is typical of earthquakes in intraplate regions (GA 2012, citing the work of Schorlemmer *et al.* 2005). Independent regional specific studies identified *b*-values of 0.88 for Australia (Allen *et al.* 2004), 0.92 for the Indian sub-continent (Jaiswal and Sinha 2006, 2007), 0.91 for New Madrid, Eastern North America (Stein and Newman 2004) and 0.90 for Africa (Heety 2011). All these regions are predominantly intraplate in tectonic terms and a *b*-value of 0.9 is considered to be a reasonable assumption for the purpose of this study. Given that only intraplate events of M5 or

higher magnitudes have been counted and that $M > 6$ events are rare (though possible) the total hazard as expressed in the form of an elastic response spectrum for use in design would be correlated well with the number of $M > 5$ events. Thus, predictions from PSHA of broad source models would not be as sensitive to the b -value assumed in the analysis as predictions from small source models which usually rely heavily on the use of statistics of the occurrence of minor tremors, and an estimated b -value, to infer the rate of occurrence of ($M > 5$) events that are of engineering significance.

In view of the generally very low rate of occurrence of intraplate earthquakes the number of events counted was normalised to a standard land area of 1,000,000 square kilometres (sq km) which is consistent with conventions adopted by Bird *et al.* (2010) and by Bergman and Solomon (1980). For example, the listing of historical earthquakes occurring in the eastern part of Australia (shaded in Fig. 1(a)) over the past 50 years was sourced from the website of Geoscience Australia (2015). Fifteen earthquake events exceeding magnitude 5 (following conversion to the scale of moment magnitude) were identified from the list and were located (Fig. 1(b)). Given that the land size of the study area was 2,444,090 sq km, the normalised count is accordingly rounded off to the value of 6 (being 15 divided by 2.44). Similar counting was carried out for the whole of Australia and a normalised count value of 6 was also found. The larger the land area, the larger the amount of data is collected for a given duration of exposure. Thus, the Australian database has great significance in this study and much is attributed to the size of its landmass which is wholly within a tectonic plate and is remote from any plate margins.

The counting was then repeated for a number of countries (or part of a country) that are away from any tectonic plate boundary over four continents around the globe as listed in Table 1. Only earthquakes occurring on land have been included in the counting given that there is a significantly lower average rate of occurrence of intraplate earthquakes in oceans (as revealed in the later part of this section). The number of events is divided by the land area of the respective country in order that the normalised figures from each of the listed countries can be compared. All earthquake magnitudes of the historical events have been converted to the moment magnitude scale as per conversion relationship provided in McCalpin (2009). No correction for aftershocks has been applied given that the number of aftershocks of intraplate earthquakes exceeding $M5$ is not significant.

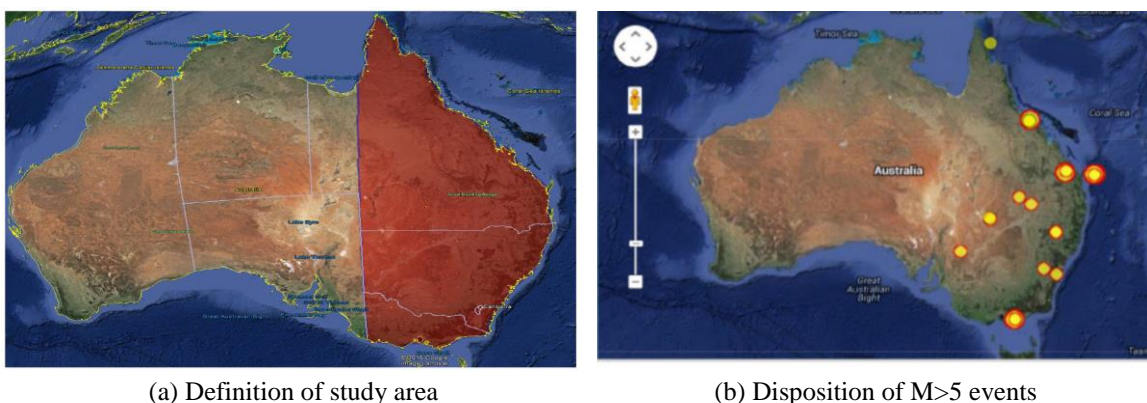


Fig. 1 Eastern Australia (shaded part) and location of $M > 5$ events in the past 50 years (data collected and images reproduced from Google Earth)

Interestingly, the normalised event counts as presented in Table 1 are all very consistent. In most cases individual normalised event counts are in the range 4 - 6 (except for a couple of countries where the total counts are considered too small to have statistical significance). It can be shown that the normalised event count based on combining countries in western Europe would not exceed this limit provided that areas close to the tectonic plate margin (in northern Italy, for example) have been excluded. However, there are areas (namely South China, the British Isles and the Korean peninsula) where individual normalised event counts are in the range 9 - 11. It is not the intention of Table 1 to make the suggestion that countries that have been identified with a higher normalised number of event count (e.g., *Eastern and Central China, Korean Peninsular*) would necessarily be having a higher underlying rate of recurrence as the displayed variations might well be the result of the smallness of the sample (i.e., small area of landmass). The presented statistics of event counts is not sufficient to indicate an exact global average value. However, it is clear that this global average value is within the range of **5 - 10**. A parameter K_D is introduced herein to represent the rate of recurrence of intraplate events where $K_D=1$ refers to five $M>5$ events occurring in an area of 1,000,000 sq km in the past 50 years, and $K_D=2$ refers to ten such events. Amid the uncertainties and lack of adequate local information, it is prudent to err on the safe side. Thus, “**10**” (i.e., $K_D=2$) is a reasonable, and conservative, normalised event count to assume provided that (validated) local data of earthquake occurrence does not infer a higher value.

The rate of seismic activity is conventionally defined using the *Gutenberg-Richter* magnitude recurrence relationship of the form

$$\log_{10} N(M) = a - bM \quad (1a)$$

Table 1 Number of $M \geq 5$ intraplate earthquake events on land in a 50 year period

Country	Land Area (10^6 km 2)	N($M \geq 5$) in 50 years [Recorded Number]	N($M \geq 5$) in 50 years [Recorded Number Normalised to 1,000,000 km 2]
Brazil ₂	8.52	33	4
Australia (whole continent) ₁	7.69	45	6
Australia (eastern states only)	2.44	15	6
Eastern US ₃	2.29	13	5 - 6
Eastern & Central China ₂	1.55	14	9
France ₄	0.67	4	6
Southern India ₅	0.64	3	5
Germany ₄	0.36	1	3
British Isles ₄	0.32	3	9 - 10
Korean Peninsula	0.26	3	11
Peninsular Malaysia	0.13	<1	<1

1. Data were obtained from GA (Geoscience Australia) earthquake catalogue, web reference: <http://www.ga.gov.au/earthquakes/>

2. Data were obtained from PAGER-CAT earthquake catalogue, reference: Allen *et al.* (2009)

3. Data were obtained from CEUS earthquake catalogue, web reference: <http://www.ceus-ssc.com/>

4. Data were obtained from EMEC earthquake catalogue, reference: Grünthal & Wahlström (2012)

5. Data were obtained from reference: NDMA (2011)

or

$$\log_{10} N(M) = a_5 - b(M - 5) \quad (1b)$$

where $N(M)$ may be defined as the expected number of earthquakes $\geq M$ occurring within an area of 1,000,000 km² over a 50-year period, and a , a_5 and b are defined as the seismic constants.

For $K_D=1$, $a_5=0.7$ or $a=5.2$ (being $0.7+0.9 \times 5$) assuming $b=0.9$. Similarly, for $K_D=2$, $a=5.5$. Given the seismic constants and a suite of representative ground motion prediction expressions (GMPEs) PSHA can be undertaken to quantify ground motion intensities in probabilistic terms as demonstrated in the later sections of the paper.

An alternative method of surveying the rate of recurrence of intraplate earthquakes on the global scale involves using the *Global Strain Rate Model* of Bird *et al.* (2010). Tectonic movement is classified by this model into four deformation regimes namely: (i) *Subduction*; (ii) *Diffuse Oceanic*; (iii) *Ridge-Transform*; and (iv) *Continental*. The rate of recurrence of earthquake events in the four deformation regimes was modelled using the *Seismic Hazard Inferred From Tectonics* (SHIFT) approach which involves monitoring tectonic activities through analysis of data from *Global Position System* (GPS) geodetic velocity measurements. Earthquakes generated from (all land and sea) areas that are not part of any of these deformation regimes are classified as intraplate earthquakes. The rate of intraplate activities around the globe which represents only 2.7% of shallow seismicity was modelled by taking an empirical-averaging method. An average activity rate based on the number of events (of magnitude equal to and exceeding 5.66) per *square meter* and per *second* was estimated at 4.27×10^{-22} which is translated into 0.67 (or $10^{-0.17}$) number of events in an area of 1,000,000 km² over a 50-year period. This occurrence rate estimate is for all intraplate earthquakes occurring on both land and sea around the globe.

As shown on the *Rate Map* of Bird *et al.* (2010) the global average recurrence rate of intraplate earthquakes covering both land and sea is an order of magnitude lower than that identified for activities in *Diffuse Oceanic* (ii) regimes; two orders of magnitude lower than *Continental* (iv) regimes; and three orders of magnitude lower than the *Subduction* (i) and *Ridge Transform* (iii) regimes. Thus, the average rate of recurrence of intraplate earthquakes as inferred from the global catalogue dataset for intraplate regions is well aligned with those inferred from GPS geodetic velocity measurements for high seismic regions. This inferred seismicity can be represented in the Gutenberg-Richter form as $a=4.9$ (being $-0.17+0.9 \times 5.66$) assuming $b=0.9$. The rate of recurrence of $M>5$ events is accordingly **2 - 3** in an area of 1,000,000 km² and exposure period of 50 years.

The normalised event count of **2 - 3** for both land and sea is somewhat lower than the figures presented in Fig. 1 (being typically in the range **5 - 6**) which are based on event counts on land. It is noted that studies of intraplate seismicity in oceanic regions over the period 1963 - 1980 by Bergman and Solomon (1980) revealed as few as **1 - 2** intraplate events occurring in oceans (based on the full catalogue) when normalised to an area of 1,000,000 km² and exposure period of 50 years. Oceanic areas adjacent to India have the highest count (3 - 4) whereas areas adjacent to Africa have the lowest count (<1). The normalised counts of events on land (continents) alone as listed in Table 1 is therefore expected to be somewhat higher than the **2 - 3** inferred from the *Global Strain Rate* model of Bird *et al.* (2010). In summary, seismicity estimates on the global scale as represented by Table 1 and the Bird model are consistent.

The *broad source zone modelling* approach assuming a global average rate of recurrence of intraplate activities (as derived in this section) draws upon the vast landmass of a number of stable continental (intraplate) areas around the globe to compensate for their individual lower rates of seismic activity. This is expected to provide a much more robust representation of seismic activity

compared with locally developed models in stable continental regions. Essentially, the modelling approach as described herein serves to reduce uncertainties as much as possible in the prediction of events exceeding M5. Given that the great majority of intraplate earthquakes are only up to M5.5, and that the predicted hazards associated with a $M > 6$ event has only very minor contributions to the total hazard (as demonstrated later in the paper), the accuracies of the model predictions would not be compromised a great deal by uncertainties in the prediction of the b -value.

However, the rate of occurrence of intraplate earthquakes is actually not uniform in space and time (contrary to the assumption of the *broad source zone model*). Seismicity within a region can also be subject to both spatial and episodic variations (Leonard *et al.* 2007). In the absence of a definitive emerging seismicity pattern there is a great deal of uncertainty over the size and location of the earthquake generating sources. Thus, the *broad source zone model* presented herein is primarily intended to set a minimum threshold value of intraplate hazard and not be used to accurately predict the spatial, or temporal, distribution of seismic hazard within a region.

There are situations where the rate of earthquake recurrence in an intraplate area may exceed the predicted global average. For example, the spatial distribution of earthquake activities in Central and Eastern United States (CEUS) show that some 80 - 90% of the epicentres of earthquakes exceeding M5 were located within only one-third of the area according to results of a regional seismological survey study (Kafka 2007). These relatively active parts of the CEUS have 2.5 - 3 times more earthquakes per unit area than that estimated by the assumption of uniform seismicity across the entire region of CEUS and the PSHA method can be used with some confidence given the high number of seismic events recorded. In contrast, the *broad source zone modelling* approach based on the estimated average global rate of recurrence of intraplate earthquakes is potentially of good practical value in other parts of the world where a reliable prediction of threshold hazard cannot be derived from the analysis of local seismicity data alone.

3. Probabilistic seismic hazard assessment based on predicted rate of recurrences

This section is concerned with explaining how ground motion intensities are derived as function of the return period and parameters which characterise a broad source zone in the presented simplified approach. The analysis of seismic hazard at a pre-defined location in an area where uniform distribution of seismic activities is assumed only need to consider one source zone which can be circular and centred at the site under consideration (Fig. 2). R_{\max} is the distance limit beyond which the intensity of the transmitted ground motions is deemed negligible. In this study the value of R_{\max} was taken as 200 km. The probability density function for source-site distance R (spatial distribution of seismicity) within the source zone can be expressed as follows

$$f(R) = \frac{2R}{R_{\max}^2} \quad (2)$$

The earthquake recurrence relationship assuming a doubly-truncated exponential function can be expressed as follows

$$N(M) = \nu \frac{\exp[-\beta(M - M_{\min})] - \exp[-\beta(M_{\max} - M_{\min})]}{1 - \exp[-\beta(M_{\max} - M_{\min})]} \quad (3a)$$

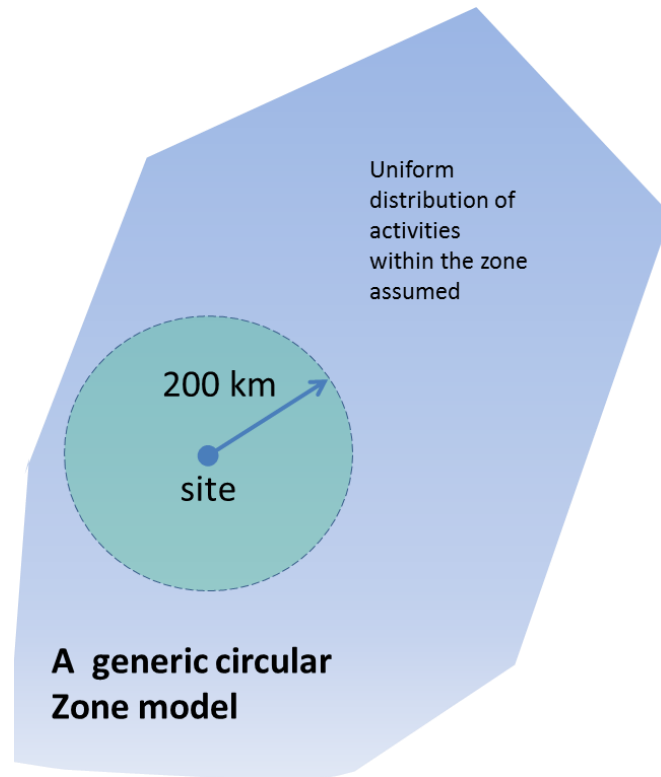


Fig. 2 Circular source model for PSHA assuming uniform distribution of seismicity

where $N(M)$ is the number of earthquakes with magnitude greater than M , occurring in a fixed time interval and within the circular source area of radius R_{\max} . ν is the total number of earthquakes with magnitude greater than M_{\min} , occurring in a fixed time interval and within the circular source area. $\beta = 2.3b$, in which b is the slope of the Gutenberg-Richter relationship. The corresponding probability density function is defined as follows

$$f(M) = \frac{\beta \exp[-\beta(M - M_{\min})]}{1 - \exp[-\beta(M_{\max} - M_{\min})]} \quad (3b)$$

For every combination of M and R , seismic intensities are predicted by employing suitable ground motion prediction equations (GMPEs). Finally, the total seismic hazard of the site encompassing all the considered M - R combinations can be computed using the conventional *Cornell-McGuire* approach (Cornell 1968, McGuire 1976) which is represented by the following integral

$$P[Z > z] = \nu \int_R \int_M P[Z > z | M, R] f(M) f(R) dM dR \quad (4)$$

The implementation of the computational algorithm on an EXCEL spreadsheet based on subdividing the circular source into ring sub-sources to facilitate analyses on a spreadsheet has been demonstrated in Lam *et al.* (2015) and a summary presented in the appendix of this paper.

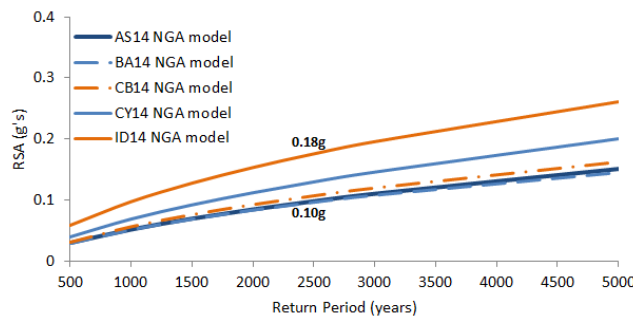
4. Response spectra derived from published Ground Motion Models

4.1 Use of conventional ground motion models developed from strong motion data

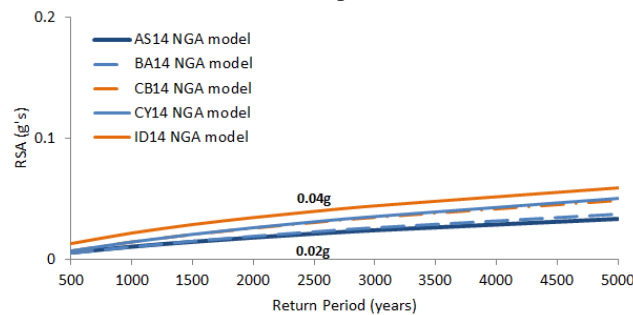
Once the recurrence behaviour of local earthquakes has been modelled suitable ground motion relationships have to be selected as part of the *PSHA* procedure. The great majority of strong motion data used in most empirical ground motion prediction equations (GMPEs) are from tectonically active (high seismicity) regions. *Next Generation Attenuation* models of Western North America (*NGA-West2*) were developed by sourcing the service of five reputable groups of researchers to work on a common pool of strong motion data that have been collected in tectonically active regions. The literature references for the five GMPEs along with their acronyms are listed in Table 2.

Table 2 Literature references and acronyms to conventional ground motion models

Literature citations	Acronyms in legends	Remarks
Abrahamson <i>et al.</i> (2014)	AS14	Earthquake Spectra v30
Boore <i>et al.</i> (2014)	BA14	Earthquake Spectra v30
Campbell and Bozorgnia (2014)	CB 14	Earthquake Spectra v30
Chiou and Youngs (2014)	CY 14	Earthquake Spectra v30
Idriss (2014)	ID 14	Earthquake Spectra v30

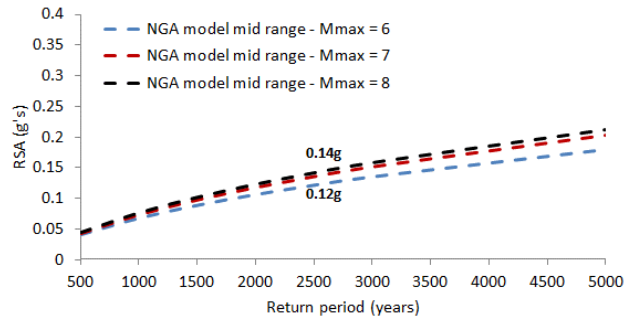


(a) 0.3 s period

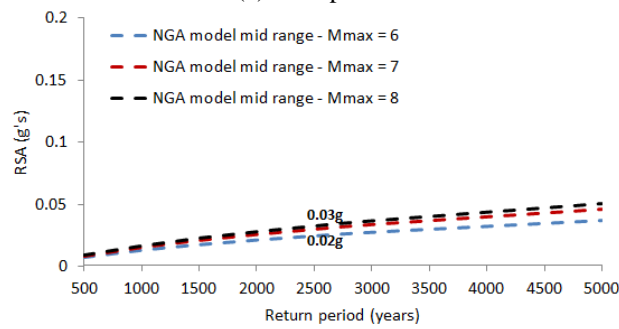


(b) 1.0 s period

Fig. 3 Results of PSHA on rock for $\text{Log}_{10}N=5.2-0.9M$ (i.e., $K_D=1$) for *NGA-West2* $M_{\min}=4$ and $M_{\max}=7$ (response spectral values are based on 5% viscous damping)

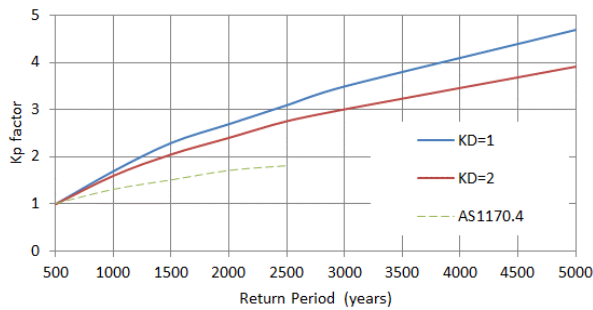


(a) 0.3 s period

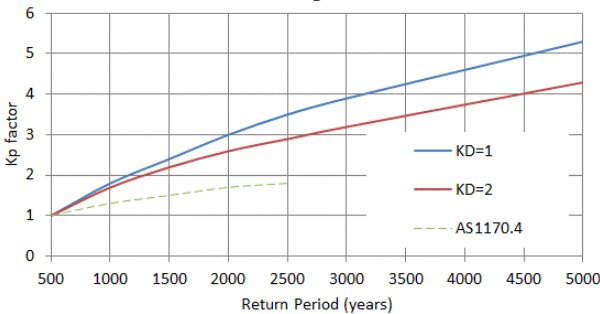


(b) 1.0 s period

Fig. 4 Results of PSHA on rock for $\text{Log}_{10}N=5.5-0.9M$ (i.e., $K_D=2$) $M_{min}=4$ for NGA-West2 (response spectral values are based on 5% viscous damping)



(a) 0.3 s period



(b) 1.0 s period

Fig. 5 Return Period Factor $M_{min}=4$ and $M_{max}=7$ (response spectral values are based on 5% viscous damping)

Results from PSHA as derived using Eqs. (2)-(4) can be presented in the form of elastic response spectral acceleration (*RSA*) values as function of return period for a given level of seismicity defined in the Gutenberg Richter form (Eq. (1)). *RSA* (*g*'s) values have been calculated for each of the five NGA-West2 models at various natural periods. Median predictions of the *RSA* (*g*'s) values are presented in Figs. 3(a) and 3(b) for periods of 0.3s and 1.0s based on the rate of recurrence as defined by: $a=5.2$ and $b=0.9$ (i.e., $K_D=1$).

Predictions shown in Figs. 3(a) and 3(b) for the individual models are broadly consistent and particularly for higher natural periods (i.e., 1.0 s) (Fig. 3(b)). However, larger inter-model discrepancies are shown at lower natural periods (i.e., 0.3 s) (Fig. 3(a)) even when a common pool of data has been employed in the model development.

Sensitivity analyses have been carried out to reveal differences in the estimated hazard when different magnitude ranges are considered. It is shown in Figs. 4(a) and 4(b) that contributions by earthquake scenarios exceeding M6, and M7, were generally insignificant in low seismicity conditions.

Sensitivity analyses have also been undertaken to track the changes in the *RSA* values as the K_D value of **1** was increased to **2** (corresponding to the doubling of the rate of recurrence of $M>5$ events for a given area of landmass over a fixed period). Interestingly, the corresponding increase in *RSA* values at a return period of 2475 years was only about 37.5%.

Results have been calculated for return periods of up to 5000 years and presented in Figs. 5(a) and 5(b) in the form of return period (K_p) factors and compared with recommendations by codes of practices (e.g., AS1170.4, 2007). It is shown that the value of K_p for a return period of 2475 years is of the order of 3.0 in comparison with the code specified value of 1.8. K_p values calculated for 0.3 s and 1.0 s periods are shown to be very similar.

4.2 Use of NGA-East Ground Motion Models

Results presented in Section 4.1 were derived from Ground Motion Models (GMMs) that were developed mainly from strong motion accelerogram data collected in tectonically active regions. Thus, results of *PSHA* based on the use of those GMMs cannot automatically be taken to be representative of places located in tectonically stable regions such as *Central North America*, *Australia*, and *Southern India*. Thus, alternative GMMs that have been developed from an intraplate seismo-tectonic environment need to be sought for realistic hazard predictions in areas of low-to-moderate seismicity.

The *Next Generation Attenuation of eastern North American (NGA-East)* database comprises 29000 records from 81 intraplate earthquake events that were recorded from 1379 stations (PEER 2015/04). Ground Motion Models (GMMs) derived from this database (which is at present the most elaborate database of intraplate earthquakes) should be taken to be indicative of the intrinsic source characteristics of earthquakes generated in an intraplate environment. A literature review of seismological studies of ground motion models of *Eastern North America* (ENA) identified some 40 models that were developed in the period 1983-2014. A subset of 22 models were selected based on quality and age of data. Further screening managed to reduce the 22 models into 6 representative models (PEER 2015/04). The acronyms for the six selected published ground motion models (Table 3) are namely: (i) AB95 (ii) SGD02 (iii) A04* (iv) BCA10d (v) BS11 (vi) AB14*. Models labelled with an asterisk feature a geometrical attenuation factor of $R^{-1.3}$ within about 50 km site-source distance as opposed to the conventional factor of R^{-1} .

The mainstream methodology that has been adopted for deriving GMMs for *NGA-East* is

stochastic simulations of the seismological model. The credibility of a proposed GMM is best tested by matching simulations from one of the seismological models with representative recorded field data. The matching is often not straightforward because of trade-offs between various factors of the attenuation relationship in order that solutions based on the best match are non-unique. The *source factor* in the seismological model controls properties of seismic waves radiated from the source of an earthquake, and is mainly characterised by the *stress parameter* (which has also been described as “*stress drop*”) which is indicative of the rate of fault slip and hence the rate of energy release in an earthquake. The higher the value of the *stress parameter* the higher the slip rate/energy release and the higher is the frequency content of the radiative shear waves which are then translated into earthquake ground motions as the wavefront reaches the ground surface. Earthquakes in tectonically active regions (i.e., interplate earthquakes) usually have *stress parameter* values lower than 100 bars. In contrast, much higher *stress parameter* values have been found with intraplate earthquakes. The frequency content of an earthquake as reflected in RSA values at low periods in particular are controlled by the *stress parameter* value.

In the evaluation work of Boore (Chapter 2 in PEER 2015/04) *stress parameter* values were calibrated in order that simulations from the respective seismological model match with individual earthquakes recorded in *Central North America* (CNA). In a calibration study involving nine intraplate earthquakes of M4.4 - M6.8 recorded in CNA that were compared with published point source simulation models of Atkinson and Boore (1995), Boatwright and Seekins (2011) and Boore *et al.* (2010) (abbreviated herein as AB95, BS11 and BCA10d respectively) very well constrained geometrical mean calibrated *stress parameter* values of 137 bars, 173 bars and 185 bars were found. The calibrated *stress parameter* values of any individual earthquake never exceeded 400 bars with these point source models (except for the anomalous *Saguenay* earthquake of 1988). The other two models marked with an asterisk featured exceptionally high *stress parameter* values of 900 bars - 1200 bars to compensate for the rapid diminution of energy enforced by the $R^{-1.3}$ geometrical attenuation factor. Given that *stress parameter* only controls the high frequency behaviour of radiated seismic waves, the lower frequency wave components are not as well compensated. Thus, GMMs in this category has been found to be understating ground motions at period of 1 s and above.

An independently developed GMM (*DASG15*) as introduced in Chapter 3 of PEER 2015/04 has also been constructed from a seismological model that had been derived (more recently) from the broadband inversion of the *NGA-East* database. The inversions involved 1133 recordings from 53 earthquakes recorded from 41 stations (but only two $M > 5$ events: M5.8 and M5.1). The *DASG15* model was not within the scope of the evaluation study by Boore (Chapter 2 in PEER 2015/04). The calibrated stress parameter value of 120 bars with the *DASG15* model (for M5.5 and above) is in good agreement with the range of stress parameter values reported in the above for the AB95, BS11 and BCA10d GMMs. An interesting finding revealed from the *DASG* study is the stepped increase in the calibrated stress parameter value as the value of M crosses over the M5 limit. This phenomenon is well established with the *NGA-West2* data (which shows such a stepped increase from 26 bars to 53 bars) and has been adapted for use in the point source simulation of intraplate earthquakes under *DASG15* (which assumes a similar stepped increase from 60 bars to 120 bars). The shortcomings of extrapolating ground motion behaviour with magnitude scales simply by regression analysis are well highlighted.

Other models from reputable sources including the hybrid empirical models (*PZCT15**), the Central and Eastern North America (CENA) finite fault models (e.g., *SP15**), and the traditional empirical model of *ANC15* that were derived from macro-seismicity data (that are introduced in

Chapters 5, 7 and 8 of PEER 2015/04) have also been included in the investigatory study. The *PZCT15** and the *SP15** GMMs which are also labelled with an asterisk feature the use of the $R^{-1.3}$ as the geometrical attenuation factor for R up to 50 km.

Results of PSHA showing *RSA* values at 0.3 s and 1.0 s based on a selection of GMMs of *NGA-East* are superposed on the range of predictions based on the GMMs of *NGA-West2* (Figs. 6(a)-6(b)). Clearly, GMMs namely *AB95* and *DASG15* are more robust than the *SP15** and *PZCT15** models in view of inter-model consistencies. An earlier independent review of GMMs developed for use in ENA by Ogwen and Cramer (2014) also ranked *AB95* favorably in view of consistencies between the model predictions and field recordings. There is no intention to identify which GMMs are the more “correct” GMM for CENA. It so happens that predictions from the *AB95* and the *DASG15* GMMs of *NGA-East* are overall comparable with predictions from the *NGA-West2* and only marginally higher at 0.3 s.

Table 3 A selection of ground motion models for use in *tectonically stable regions*

Literature citations	Acronyms in legends	Remarks
Atkinson and Boore (1995)	AB95	BSSA article
Pezeshk, Zandieh, Campbell and Tavakoli (2015)	PZCT15	PEER report 2015/04
Darragh <i>et al.</i> (PEER, 2015)	DASG15	PEER report 2015/04
Shahjouei and Pezeskh (PEER, 2015)	SP15	PEER report 2015/04
Al Noman and Cramer (PEER, 2015)	ANC15	PEER report 2015/04
Silva, Gregor and Darragh (2002)	SGD02	PEA report 2002
Atkinson (2004)	A04	BSSA article
Boore, Campbell and Atkinson (2010)	BCA10d	BSSA article
Boatwright and Seekins (2011)	BS11	BSSA article
Atkinson and Boore (2014)	AB14	BSSA article

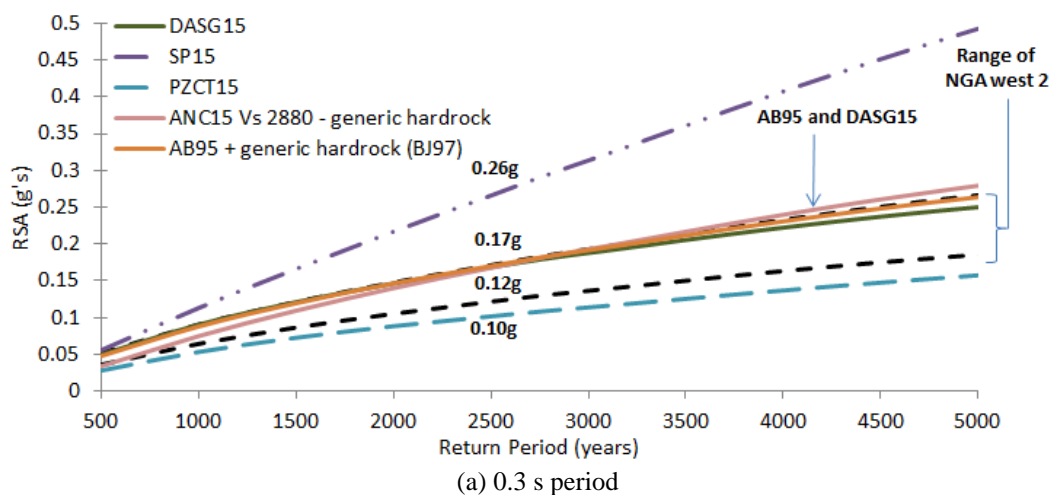
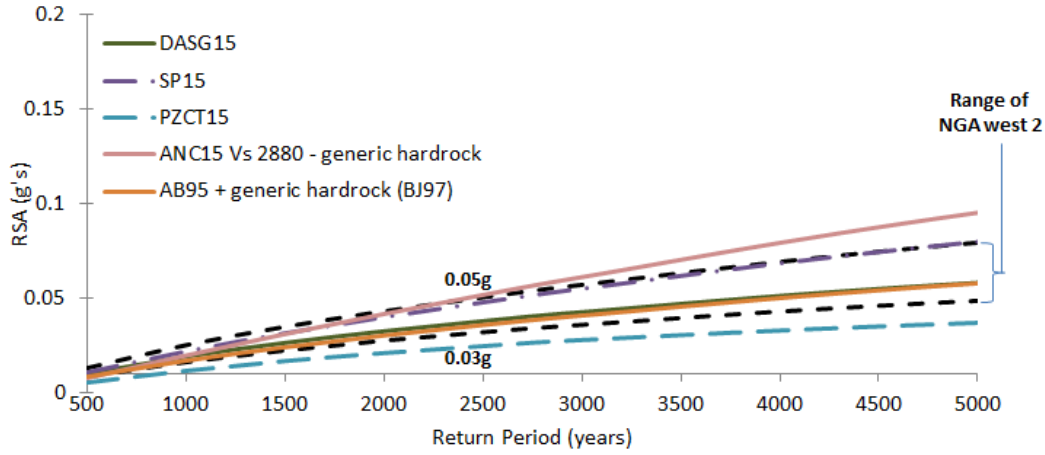


Fig. 6 Results of PSHA on rock for $\text{Log}_{10}N=5.5-0.9M$ (i.e., $K_D=2$) for *NGA-East* $M_{\min}=5$ and $M_{\max}=7$ (response spectral values are based on 5% viscous damping)



(b) 1.0 s period
Fig. 6 Continued

4.3 Use of ground motion and crustal models for non-cratonic conditions

Crustal conditions of tectonically stable regions can either be *cratonic* or *non-cratonic* as shown in Table 4 for a range of regions around the world. It is shown that two tectonically stable regions can have different crustal classifications. For example, the crustal conditions in *Southeastern Australia* and *Peninsular Malaysia* are much closer to that of *California* than to *Central North America*. Most ground motion data that have been used to develop ground motion models of *NGA-East* were collected from the cratonic crustal region of *Central North America* (i.e., region 2 as defined in chapter 1 of PEER2015/04). However, it is a fallacy to consider *NGA-East* models to be automatically suited for applications across all intraplate regions.

Adapting GMMs for use in low-to-moderate seismicity countries must take into account factors controlling the (a) waves generation behaviour at the source of the earthquake in a given tectonic

Table 4 Countries identified with different tectonic and crustal classifications

Tectonic Classification Crustal Classification	Tectonically Active	Tectonically Stable
Non-Cratonic	<i>Western North America</i> <i>Western South America</i> <i>Indonesia</i> <i>New Zealand</i> <i>Japan</i> Most parts of <i>Southern Europe</i> and <i>Middle East</i>	<i>Southeastern Australia, Central and</i> <i>Southern China and Peninsular</i> <i>Malaysia</i>
Cratonic	-	<i>Central North America</i> Parts of <i>Eastern South America,</i> <i>Central and Western Australia,</i> <i>Scandinavia.</i> <i>Southern India and Sri Lanka.</i>

setting and (b) waves modification behaviour of the earth (basement rock) crusts which are not to be confused with the modification behaviour of near-surface sediments. Most of the GMMs of *NGA-East* as presented in Section 4.2 are implicitly representative of *cratonic* conditions which are identified with negligible modifications to seismic waves as they propagate up the crustal layers. In contrast, a GMM model to be adapted for use in *non-cratonic* regions requires substantial modifications to incorporate the amplification and attenuation of waves within the upper 3 - 4 km of the earth crust.

The authors had experience of combining the source model of *AB95* with the (non-cratonic) crustal model of *generic rock* (Boore and Joyner, 1997 which is abbreviated herein as *BJ97*) for predicting ground motions generated by intraplate earthquakes in what has been described as the *Component Attenuation Model* framework (Lam *et al.* 2000, 2010). The crustal model of *BJ97* has since been made more versatile by parameterising the V_s (30 m) value as an input parameter (Chandler *et al.* 2005, Boore 2016) in order that any crustal velocity profiles that are intermediate between the classical *generic rock* and *generic hard rock* limits can be incorporated into an existing ground motion simulation framework. An alternative crustal velocity profile modelling approach has also been developed for various crustal conditions (Chandler *et al.* 2005). Simulated *RSA* values for the *non-cratonic* version of *AB95* based on the classical *generic rock* class of Boore and Joyner (1997) is representative of *non-cratonic* regions. The credibility of those simulations under the framework of the *Component Attenuation Model* has been established through demonstrating agreement with field observations from different countries (expressed in the form of Intensity data) as shown in some earlier journal publications by the authors and co-workers over the years (e.g., Chandler and Lam 2002, Chandler *et al.* 2006, Lam *et al.* 2003, 2006, Tsang *et al.* 2010, Yaghmaei-Sabegh and Lam 2010). Predictions by the (*non-cratonic*) model are shown in Fig. 7(a) and 7(b) to be significantly higher than the upper limit of predictions by the *NGA-West2* models. Thus, the use of *NGA-West2* models or *NGA-East* models in PSHA could result in the seismic hazard understated in places like *Southeastern Australia* and *Peninsular Malaysia*.

5. Case study for illustrating the use of proposed minimum loading model

In the case study of *Peninsular Malaysia*, the *broad source zone* modelling approach was applied. The recurrence modelling of potentially destructive earthquakes was predicted directly by counting the number of $M > 5$ event count (defined herein as N_5) in the 50-year period over an aggregated land area of 272,000 sq km. Given that the tectonic and crustal classification of the neighboring state of *Sarawak* and the western part of *Sabah* are similar to that of *Peninsular Malaysia*, the three areas have been combined in the event counting. The event count of 3 is translated to 11 as the area of the landmass is normalised to 1 million sq km (refer Table 5).

This frequency figure is consistent with statistics of historical earthquakes observed in the intraplate regions of the *Korean Peninsular* and *Eastern China* as presented in Section 2 of this paper. The recurrence behaviour can be represented by the following expression of the *Gutenberg-Richter* form (Eq. (5)) based on a pre-determined b -value of 0.9 and a (rounded-off) normalised event count of $N_5=10$ which corresponds to $K_D=2$ which is consistent with recommendations made in Section 2 of the paper.

$$\text{Log}_{10}N = 5.5 - 0.9M \quad (5)$$

Table 5 Listing of local $M > 5$ events in the *Peninsular, Sarawak and South-western Sabah* in the 50 year period 1966 - 2016

Region	Area of the region (sq km)	Magnitude of historical earthquake	Year of occurrence	Location of epicenter
Peninsular	130,598	*M4.6	1984	Tasik Kenyir
Sarawak	124,450	M5.3 M5.2	1994 2004	Bukit Mersing Tubau
South-western Sabah	16,951	-	-	-
Total Area =			272,000	

*Given the uncertainties in the magnitude estimation of earthquake this event has been included in the count

where N is the event count for earthquake with magnitude $> M$ over a period of 50 year period in a source area of 1 million sq km.

Given the *non-cratonic* crustal classification of *Peninsular Malaysia and Sarawak* the predictions of *RSA* can be based on the use of the *AB95-generic rock (BJ97)* model of Figs. 7(a) and 7(b). For a return period of 2475 years, a *RSA* value of approximately 0.25 g is predicted at period of 0.3s for the recurrence behaviour as defined by Eq. (5) (i.e., $K_D=2$). The effective peak ground acceleration (*EPGA*) is accordingly 0.1 g (being 0.25 g/2.5). The reference *EPGA* value based on a notional return period of 475 years (corresponding to 2/3 of predictions at 2475 years) is accordingly 0.07 g.

This paper is aimed at giving recommendations for incorporating into design codes of practices which typically stipulate response spectra in the *flat-hyperbolic* form. This common format of presenting the response spectrum for use in engineering design features the use of the response spectral acceleration at 0.3 s to define the *flat* part of the spectrum, and 1.0 s for the *hyperbolic* part. The 1st corner period (T_1) value may also be used to control the *hyperbolic* part of the spectrum; and a T_1 value of 0.3s has been found to be sufficiently conservative as it envelopes response spectral accelerations at periods exceeding 0.3 s. The *RSA* vs natural period relationships are accordingly defined by Eqs. (6a) and (6b) for a return period of 2475 years, and Eqs. (7a) and (7b) for a notional return period of 475 years. Refer also Figs. 8(a) and 8(b) for schematic diagrams defining the recommended idealised elastic design response spectra to represent the minimum loading requirements for the case study area. These response spectra only provide coverage for *acceleration* and *velocity* controlled conditions whereas the higher period part of the response spectrum for *displacement* controlled conditions can be defined in accordance with a deterministic second corner period (T_2) value. The high-period behavior of the response spectrum is beyond the scope of this paper and is the subject matter of an earlier publication of the authors (Lumantarna *et al.* 2012)

$$RSA_{0.3s}(g's) = 0.25 \quad (6a)$$

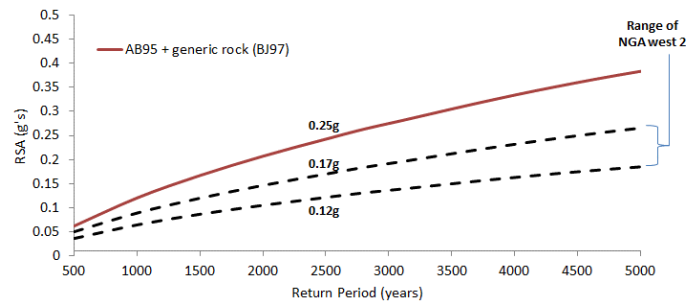
$$RSA_{0.3s}(g's) = \frac{0.075}{T} \quad (6b)$$

whichever is lesser for return period of 2475 years.

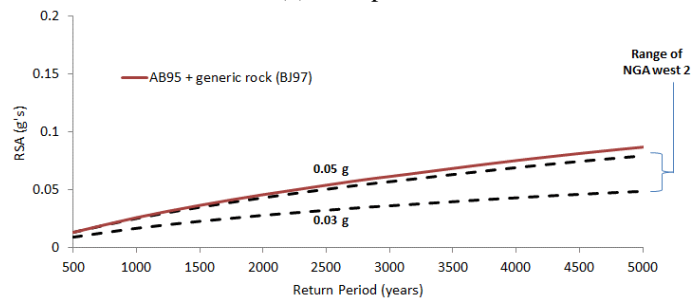
$$RSA_{0.3s}(g's) = 0.175 \tag{7a}$$

$$RSA_{0.3s}(g's) = \frac{0.0525}{T} \tag{7b}$$

whichever is lesser for return period of 475 years.

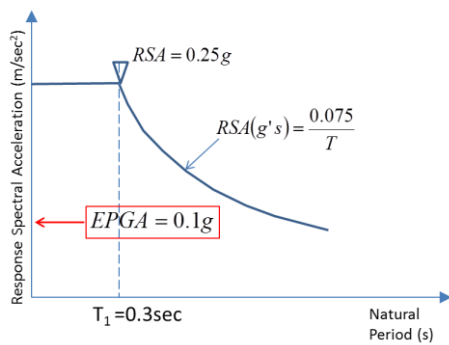


(a) 0.3 s period

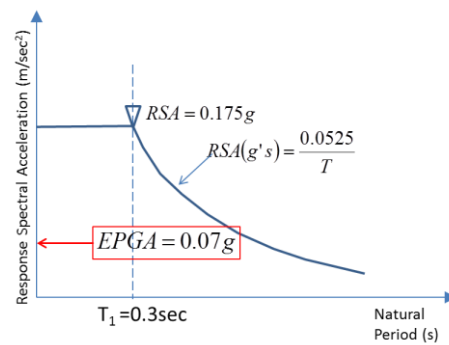


(b) 1.0 s period

Fig. 7 Results of PSHA on rock for $\text{Log}_{10}N=5.5-0.9M$ (i.e., $K_D=2$) for tectonically stable and non-cratonic conditions, $M_{\min}=5$ and $M_{\max}=7$ (response spectral values are based on 5% viscous damping)



(a) Return Period of 2475 years



(b) Notional Return Period of 475 years

Fig. 8 Idealised elastic response spectra on rock for to cover for local earthquakes in Peninsular Malaysia (response spectral values are based on 5% viscous damping)

The shortcoming of the *broad source zone* modelling approach as described is its failure to capture “hot spots” of destructive historical activities. There is the option of superimposing the modelled hazard (for the identified hot spots) on a map showing uniform hazard (that has been derived from the *broad source zone* model) in order that no area is stipulated with a level of hazard below a certain hazard threshold. The modelling methodology presented herein provides the rationale (and transparency) for quantifying this background hazard level or “background seismicity”. For the *Peninsula* in particular, and for *Sarawak* and *South-western Sabah*, no such threatening hot spot has been identified. Consequently, the level of hazard to be stipulated for this part of Malaysia can be based entirely on results derived from the *broad source zone* model.

6. Conclusions

The objective of this paper is to present the derivation of the background hazard in intraplate regions based on the rate of recurrences of earthquakes exceeding magnitude 5 observed from around the globe. The estimated background hazard was derived from results of PSHA assuming uniform spatial distribution of seismic activities. Results from the survey show that the number of intraplate earthquake events of magnitudes exceeding 5 occurring in a number of countries that are remote from any tectonic plate boundaries are typically in the range of 5-10 (i.e., $K_D=1-2$) when normalised to a standard area of 1,000,000 km² and an exposure period of 50 years. The recommended recurrence relationship for $K_D=2$ is accordingly $\text{Log}_{10}N=5.5-0.9M$. The statistics presented are generally consistent with the rate of earthquake recurrences inferred from the global strain rate model of Bird *et al.* (2010). The use of ground motion models of *NGA-West2* and *NGA-East* for *cratonic* conditions (along with wave modifications to account for conditions in *non-cratonic* regions) in *PSHA* enabled response spectral parameters to be derived in probabilistic terms for different tectonic and crustal environments. In a case study to illustrate the use of the proposed model for determining the minimum loading requirements for *Peninsular Malaysia*, an idealised elastic response spectrum corresponding to an *effective peak ground acceleration (EPGA)* value of 0.1 g is recommended for a return period of 2475 years, and 0.07 g for a notional return period of 475 years.

Acknowledgements

Contributions made by *Mehair Yacoubian* in analytical work presented in Figure 1, and that by *Daniel Looi* and *Ir Adjunct Professor MC Hee* in related collaborative work are gratefully acknowledged.

The support of the Commonwealth of Australia through the Cooperative Research Centre program is acknowledged.

References

- Abrahamson, N. and Silva, W. (2008), “Summary of the Abrahamson & Silva NGA ground-motion relations”, *Earthq. Spectra*, **24**(1), 67-97.
- Abrahamson, N., Silva, W.J. and Kamai, R. (2014), “Summary of the ASK14 ground motion relation for

- active Crustal regions”, *Earthq. Spectra*, **30**(3), 1025-1055.
- Allen, T., Gibson, G., Brown, A. and Cull J. (2004), “Depth variation of seismic source scaling relations: Implications for earthquake hazard in southern California”, *Tectonophys.*, **390**(1), 5-24.
- Allen, T., Marano, K., Earle, P.S. and Wald, D.J. (2009), “PAGER-CAT: A composite earthquake catalog for calibrating global fatality models”, *Seismol. Res. Lett.*, **80**(1), 50-56.
- Atkinson, G.M. and Boore, D.M. (1995), “Ground motion relations for eastern North America”, *Bull. Seismol. Soc. Am.*, **85**(1), 17-30.
- Atkinson, G.M. and Boore, D.M. (2014), “The attenuation of Fourier amplitudes for rock sites in eastern North America”, *Bull. Seismol. Soc. Am.*, **104**(1), 513-528.
- Atkinson, G.M. (2004), “Empirical attenuation of ground motion spectral amplitudes in southeastern Canada and the northeastern United States”, *Bull. Seismol. Soc. Am.*, **94**(3), 1079-1095.
- Australian Standard: AS 1170.4 (2007), *Structural Design Actions - Part 4 Earthquake Actions*, Standards Australia.
- Bergman, E.A. and Solomon, S.C. (1980), “Oceanic Intraplate Earthquakes: Implications for Local and Regional Intraplate Stress”, *J. Geophys. Res.*, **85**(BI0), 5389-5410.
- Bird, P., Kreemer, C. and Holt, W.E. (2010), “A Long-term Forecast of Shallow Seismicity based on the global strain rate map”, *Seismol. Res. Lett.*, **81**(2), 184-194.
- Boatwright, J. and Seekins, L. (2011) “Regional spectral analysis of three moderate earthquakes in northeastern North America”, *Bull. Seismol. Soc. Am.*, **101**(4), 1769-1782.
- Boore, D.M. and Joyner, W.B. (1997), “Site amplifications for generic rock sites”, *Bull. Seismol. Soc. Am.*, **87**(2), 327-341.
- Boore, D.M. (2016), “Determining generic velocity and density models for crustal amplification calculations, with an update of the Boore and Joyner (1997) generic site amplification for $V_s(Z) = 760$ m/s”, *Bull. Seismol. Soc. Am.*, **106**(1), 316-320.
- Boore, D.M., Campbell, K.W. and Atkinson, G.M. (2010), “Determination of stress parameters for eight well-recorded earthquakes in eastern North America”, *Bull. Seismol. Soc. Am.*, **100**(4), 1632-1645.
- Boore, D.M., Stewart, J.P., Seyhan, E. and Atkinson, G.M. (2014), “NGA-West2 equations for predicting PGA, PGV, and 5% damped PSA for shallow crustal earthquakes”, *Earthq. Spectra*, **30**(3), 1057-1085.
- Camelbeeck, T., Vanneste, K., Alexandre, P., Verbeeck, K., Petermans, T., Rosset, P., Everaerts, M., Warnant, R. and Camp, M.V. (2007), “Relevance of active faulting and seismicity studies to assessments of long-term earthquake activity and maximum magnitude in intraplate northwest Europe”, *Geolog. Soc. Am. Special Papers*, **425**, 193-224.
- Campbell, K.W. and Bozorgnia, Y. (2014), “NGA-West2 Ground Motion Model for the average horizontal components of PGA, PGV, and 5% damped linear acceleration response spectra”, *Earthq. Spectra*, **30**(3), 1087-1115.
- CEUS-SSC (Central and Eastern United States Seismic Source Characterization for Nuclear Facilities), U.S. Nuclear Regulatory Commission, U.S. Department of Energy and Electric Power Research Institute, <http://www.ceus-ssc.com/>. Accessed 2 January 2014
- Chandler, A.M. (1997), “Engineering design lessons from Kobe”, *Nat.*, **387**, 227-229.
- Chandler, A.M. and Lam, N.T.K. (2002), “Intensity attenuation relationship for the South China region and comparison with the component attenuation model”, *J. Asian Earth Sci.*, **20**(7), 775-790.
- Chandler, A.M., Lam, N.T.K. and Tsang, H.H. (2006), “Regional and local factors in attenuation modelling: Hong Kong case study”, *J. Asian Earth Sci.*, **27**(6), 892-906.
- Chandler, A.M., Lam, N.T.K. and Tsang, H.H. (2005), “Shear wave velocity modelling in crustal rock for seismic hazard analysis”, *Soil Dyn. Earthq. Eng.*, **25**(2), 167-185.
- Chiou, B.S.J. and Youngs, R.R. (2014), “Update of the Chiou and Youngs NGA model for the average horizontal component of peak ground motion and response spectra”, *Earthq. Spectra*, **30**(3), 1117-1153.
- Cornell, C.A. (1968), “Engineering seismic risk analysis”, *Bull. Seismol. Soc. Am.*, **58**(5), 1583-1606.
- Dowrick, D. (2009), *Earthquake Resistant Design and Risk Reduction*, 2nd Edition, Wiley, New York.
- Frankel, A. (1995), “Mapping seismic hazard in the central and eastern United States”, *Seismol. Res. Lett.*, **66**(4), 8-21.

- Geoscience Australia (GA) (2012), *The 2012 Australian Earthquake Hazard Map*, D.R. Burbridge (ed), Geoscience Australia publication, GeoCat 74811, Canberra.
- Geoscience Australia (GA), Earthquakes@Geoscience Australia, <http://www.ga.gov.au/earthquakes/>, Accessed 8 September 2015.
- Grünthal, G. and Wahlström, R. (2012), “The European-Mediterranean Earthquake Catalogue (EMEC) for the last millennium”, *J. Seismol.*, doi: 10.1007/s10950-012-9302-y.
- Heety, E. (2011), “Variation of b-values in the earthquake frequency-magnitude distribution with depth in the intraplate regions”, *Int. J. Basic Appl. Sci.*, **11**(6), 29-37.
- Idriss, I.M. (2014), “An NGA-West2 empirical model for estimating the horizontal spectral values generated by shallow crustal earthquakes”, *Earthq. Spectra*, **30**(3), 1155-1177.
- Jaiswal, K. and Sinha, R. (2006), “Probabilistic modeling of earthquake hazard in stable continental shield of the Indian Peninsula”, *ISIJ J. Earthq. Technol.*, **43**(3), 49-64.
- Jaiswal, K. and Sinha, R. (2007), “Spatial variation of maximum considered and design basis earthquakes in Peninsular India”, *Curr. Sci.*, **92**(5), 639-645
- Kafka, A.L. (2007), “Does seismicity delineate zones where future large earthquakes are likely to occur in intraplate environments”, *Geolog. Soc. Am. Spec. Papers*, **425**, 35-48.
- Kerr, R.A. (2011), “Seismic crystal ball proving mostly cloudy around the world”, *Science*, **332**(6032), 912-913.
- Kijko, A. and Graham, G. (1999), ““Parametric-historic” procedure for probabilistic seismic hazard analysis-Part II: assessment of seismic hazard at specified site”, *Pure Appl. Geophys.*, **154**(1), 1-22.
- Lam, N.T.K., Tsang, H.H., Lumantarna, E. and Wilson, J.L. (2015), “An alternative probabilistic seismic hazard assessment method in areas of low-to-moderate seismicity”, *Proceedings of the 2015 International Conference on Earthquakes and Structures*, Incheon, Korea, August, 2015.
- Lam, N.T.K., Wilson, J.L. and Tsang, H.H. (2010), *Modelling Earthquake Ground Motions By Stochastic Methods, Stochastic Control*, SCIYO Publisher, Chapter 23: 475 -492.
- Lam, N.T.K., Wilson, J.L., Chandler, A.M. and Hutchinson G. (2000), “Response spectral relationship for rock sites derived from the component attenuation model”, *Earthq. Earthq. Eng. Struct. Dyn.*, **29**(10), 1457-89.
- Lam, N.T.K., Sinadinovski, C., Koo, R.C.H. and Wilson, J.L. (2003), “Peak Ground Velocity modelling for Australian intraplate earthquakes”, *J. Seismol. Earthq. Eng.*, **5**(2), 11-22.
- Lam, N.T.K., Asten, M., Roberts, J., Venkatesan, S., Wilson, J.L., Chandler, A.M. and Tsang, H.H. (2006), “Generic approach for modelling earthquake hazard”, Invited paper, *J. Adv. Struct. Eng.*, **9**(1), 67-82.
- Leonard, M., Robinson, D., Allen, T., Schneider, J., Clark, D., Dhu, T. and Burbridge, D. (2007), “Toward a better model of earthquake hazard in Australia”, *Geolog. Soc. Am. Spec. Papers*, **425**, 263-283.
- Lumantarna, E., Wilson, J.L. and Lam, N.T.K. (2012), “Bi-linear displacement response spectrum model for engineering applications in low and moderate seismicity regions”, *Soil Dyn. Earthq. Eng.*, **43**, 85-96.
- McCalpin, J.P. (2009), *Earthquake magnitude scales*, In: McCalpin J.P. (ed.) *Paleoseismology*, Elsevier, London, pp. 1-3. <http://www.cascadiageo.org>. Accessed 9 January 2014.
- McGuire, R.K. (1976), *FORTTRAN program for Seismic Risk Analysis*, U.S. Geological Survey Open-file Report 76-67
- McGuire, R.K. (1993), “Computations of seismic hazard”, *Ann. Geofis.*, **36**, 181-200.
- National Disaster Manager Authority (NDMA) (2011), *Development of probabilistic seismic hazard map of India. Technical Report*, National Disaster Management Authority Government of India, New Delhi.
- Ogwen, L.P. and Cramer, C.H. (2014) “Comparing the CENA GMPEs Using NGA-East Ground Motion Database”, *Seismol. Res. Lett.*, **85** (6), 1377-1393.
- Okal, E.A. and Sweet, J.R. (2007), “Frequency-size distributions for intraplate earthquakes”, *Geolog. Soc. Am. Spec. Papers*, **425**, 59-71.
- Pacific Earthquake Engineering Center (2015), *NGA-East: median ground-motion models for the Central and Eastern North America Region*, PEER Report No. 2015/04, Pacific Earthquake Engineering Research Center, University of California, Berkeley.
- Pappin J.W., Yim P.H.I. and Koo C.H.R. (2011), “An approach for seismic design in Malaysia following the

- principles of Eurocode 8”, *IEM Jurutera Magazine*, Oct 2011, 22-28.
- Schorlemmer, D., Weimer, S. and Wyss, M. (2005), “Variations in earthquake size distribution across different stress regimes”, *Nature*, **437**(7058), 539-542.
- Silva, W.J., Gregor, N. and Darragh, R.B. (2002), “Development of regional hard rock attenuation relations for central and eastern North America”, Report to Pacific Engineering and Analysis, El Centro, C.A.
- Stein, S. and Newman, A. (2004), “Characteristic and uncharacteristic earthquakes as possible artifacts: applications to the New Madrid and Wabash seismic zones”, *Seismol. Res. Lett.*, **75**(2), 170-184.
- Stein, S., Geller, R.J. and Liu, M. (2011), “Bad assumptions or bad luck: Why earthquake hazard maps need objective testing”, *Seismol. Res. Lett.*, **82**(5), 623-626.
- Swafford, L. and Stein, S. (2007), “Limitations of the short earthquake record for seismicity and seismic hazard studies”, In: Continental Intraplate Earthquakes, *Geolog. Soc. Am. Spec. Papers*, **425**, 49-58.
- Tsang, H.H. and Chandler, A.M. (2006), “Site-specific probabilistic seismic-hazard assessment: direct amplitude-based approach”, *Bull. Seismol. Soc. Am.*, **96**(2), 392-403.
- Tsang, H.H. (2008), “Lessons Learnt from the 512 Wenchuan Earthquake: Perception of Seismic Risks”, *Proceedings of the Australian Earthquake Engineering Conference, Ballarat, Victoria, Australia*, November 21-23, 2008.
- Tsang, H.H., Sheikh, N. and Lam, N.T.K. (2010), “Regional differences in attenuation modelling for eastern China”, *J. Asian Earth Sci.*, **39**(5), 451-459.
- Tsang, H.H. (2011), “Should we design buildings for lower-probability earthquake motion?”, *Nat. Haz.*, **58**(3), 853-857.
- Tsang, H.H., Yaghmaei-Sabegh, S., Anbazhagan, P. and Sheikh, M.N. (2011), “A checking method for probabilistic seismic-hazard assessment: case studies on three cities”, *Nat. Haz.*, **58**(1), 67-84.
- Venkatesan, S., Wepitiya-Gamage, J.P., Lam, N.T.K. and Lumantarna, E. (2015), “A hybrid probabilistic seismic hazard analysis of a low and moderate seismic region: Sri Lanka - a case study”, *Proceedings of the Tenth Pacific Conference on Earthquake Engineering Building an Earthquake-Resilient Pacific*, 6-8 November 2015, Sydney, Australia.
- Wyss, M., Nekrasova, A. and Kossobokov, V. (2012), “Errors in expected human losses due to incorrect seismic hazard estimates”, *Nat. Haz.*, **62**(3), 927-935.
- Yaghmaei-Sabegh, S and Lam, N.T.K. (2010), “Ground motion modelling in Tehran based on the stochastic method”, *Soil Dyn. Earthq. Eng.*, **30**(7), 525-535.

Appendix

The land surrounding a site where uniform spatial distribution of seismicity is assumed can be divided into rings each of which can be treated as an individual earthquake source for the purpose of PSHA (Fig. A1a). The area of the ring is used for calculating the probability of earthquake events occurring (within the ring) and its distance from the site (the centre) is taken as the value of R . The conditional probability of a RSA exceeding a targeted value (RSA^*) for a given earthquake scenario expressed in terms of magnitude-distance (M-R) combination is given by the following expression as per *log-normal* distribution

$$\Pr\langle RSA \geq RSA^* | M, R \rangle = 1 - \Phi(Z^*) \quad (A1a)$$

where

$$\Phi(Z^*) = \int_{Z=-\infty}^{Z=Z^*} e^{-\frac{z^2}{2}} dz \quad (A1b)$$

Z is the zero mean log normalised ordinate

$$Z = \frac{\ln RSA - \overline{\ln RSA}}{\sigma_{\ln RSA}} \quad (A1c)$$

$\overline{\ln RSA}$ is the estimate of the mean for the given M-R combination based on the adopted ground motion prediction equation (GMPE) and $\sigma_{\ln RSA}$ is the standard deviation of the natural logarithm of the RSA values.

The annual rate of having an earthquake event with magnitude exceeding M generated by an earthquake source is

$$\lambda(M) = 10^{a-bM} \quad (A2a)$$

The annual rate of having a destructive earthquake with magnitude exceeding M_{\min} is

$$\lambda(M_{\min}) = 10^{a-bM_{\min}} \quad (A2b)$$

where $M_{\min}=4$ is assumed in this study.

As stated in the main text of the paper the value $a^*=5.2$ and $b=0.9$ (for $K_D=1$). For a circular ring

$$a = a^* + \log_{10} \left(\frac{\text{area of ring}}{\frac{1,000,000}{50}} \right) \quad (A2c)$$

where a represents the number of earthquake events occurring in a circular ring.

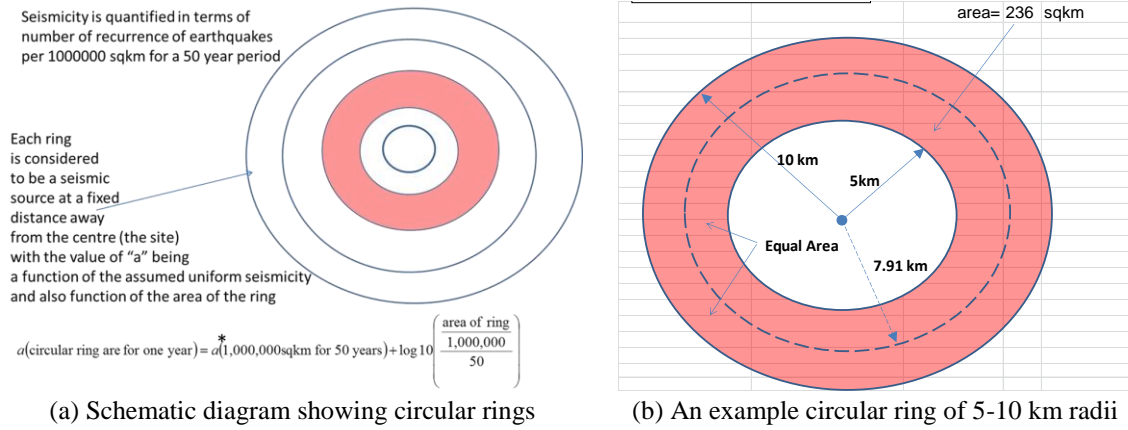


Fig. A1 Circular Ring Model for PSHA in areas of uniform seismicity

Take an example circular ring which has an area of 236 sq km and inner and outer radii of 5 km and 10 km respectively it can be shown that 50% of the area within the ring has distance from the centre exceeding the median distance of 7.91 km which is denoted as R (Fig. A1b). It can be shown from Eq. (A2c) that $a = -0.126$ when $a^* = 5.2$.

Consider a situation when a destructive earthquake magnitude (M) has occurred the probability of the magnitude of the earthquake not exceeding M is denoted as $F(M)$ where

$$F(M) = 1 - \frac{\lambda(M)}{\lambda(M_{\min})} = 1 - 10^{-b(M - M_{\min})} \tag{A2d}$$

The probability of magnitude of the earthquake falling within the bin $M_i - M_{i+1}$ is $F(M_i) - F(M_{i+1})$. The conditional probability of a response spectral acceleration (RSA) exceeding a targeted value (RSA^*) for a given earthquake of magnitude falling within the bin $M_i - M_{i+1}$ is

$$\Pr(RSA \geq RSA^*) = \lambda(M_{\min}) \times [F(M_i) - F(M_{i+1})] \times \Pr(RSA \geq RSA^* | M, R) \tag{A2e}$$

where, $M = 1/2 (M_i + M_{i+1})$, $R = 7.91$ km for the example circular ring.

Result obtained from Eq. (A2e) are to be aggregated for all distance bins (up to 200 km) and magnitude bins within the range of $M_{\min} = 4$ to $M_{\max} = 7$ which is a reasonable assumption to make for continental regions that are remote from any tectonic plate boundaries such as Australia. The mathematical expression for the aggregation can be written as follows

$$\Pr(RSA \geq RSA^*) = \sum_j \sum_i \lambda_j(M_{\min}) \times [F(M_i) - F(M_{i+1})] \times \Pr(RSA \geq RSA^* | M, R_j) \tag{A2f}$$

where subscript i and $i+1$ denote the magnitude range and j denotes the median distance of a circular ring.

Finally, the Return Period (RP) for any given value of RSA^* is accordingly taken as the reciprocal of the calculated value of $\Pr(RSA \geq RSA^*)$ as shown by Eq. (A2g)

$$RP = \frac{1}{\Pr(RSA \geq RSA^*)} \tag{A2g}$$